9388–9397 *Nucleic Acids Research, 2017, Vol. 45, No. 16* *Published online 27 June 2017*
doi: 10.1093/nar/gkx563

Cohesin acetyltransferase Esco2 regulates SAC and kinetochore functions via maintaining H4K16 acetylation during mouse oocyte meiosis

Yajuan Lu, Xiaoxin Dai, Mianqun Zhang, Yilong Miao, Changyin Zhou, Zhaokang Cui and Bo Xiong*

College of Animal Science and Technology, Nanjing Agricultural University, Nanjing 210095, China

Received March 22, 2017; Revised June 13, 2017; Editorial Decision June 15, 2017; Accepted June 19, 2017

ABSTRACT

Sister chromatid cohesion, mediated by cohesin complex and established by the acetyltransferases Esco1 and Esco2, is essential for faithful chromosome segregation. Mutations in Esco2 cause Roberts syndrome, a developmental disease characterized by severe prenatal retardation as well as limb and facial abnormalities. However, its exact roles during oocyte meiosis have not clearly defined. Here, we report that Esco2 localizes to the chromosomes during oocyte meiotic maturation. Depletion of Esco2 by morpholino microinjection leads to the precocious polar body extrusion, the escape of metaphase I arrest induced by nocodazole treatment and the loss of BubR1 from kinetochores, indicative of inactivated SAC. Furthermore, depletion of Esco2 causes a severely impaired spindle assembly and chromosome alignment, accompanied by the remarkably elevated incidence of defective kinetochore-microtubule attachments which consequently lead to the generation of aneuploid eggs. Notably, we find that the involvement of Esco2 in SAC and kinetochore functions is mediated by its binding to histone H4 and acetylation of H4K16 both *in vivo* and *in vitro*. Thus, our data assign a novel meiotic function to Esco2 beyond its role in the cohesion establishment during mouse oocyte meiosis.

INTRODUCTION

Cohesin is a multi-subunit protein complex which appears to form a ring that can encircle DNA (1). This complex is composed of four subunits: Smc1, Smc3, Rad21 and SA1 or SA2 (2,3). Cohesin and its regulatory proteins function in an essential pathway enabling proper cohesion, segregation of sister chromatids, double-strand break repair and transcriptional regulation (4). Cohesion is established in S phase at which time sister chromatids are generated by DNA replication and remain linked until their separation in anaphase. The establishment of cohesion is thought to be associated with the acetylation of the Smc3 subunit (5–8). In yeast, Smc3 acetylation is essential for viability and depends on an evolutionary conserved acetyltransferase, Eco1 (9,10). Mammalian genomes encode two Eco1 orthologs, Esco1 and Esco2 (11), both of which have been shown to acetylate Smc3 (12).

Mutations in Esco2 have been shown to cause Roberts syndrome in humans (9) that is characterized phenotypically by symmetrical limb reduction, craniofacial anomalies, growth retardation, mental retardation, cardiac and renal abnormalities, as well as spontaneous abortions in females (13). Deficiency in *Esco2* leads to the termination of mouse embryogenesis in the pre-implantation period (14). In addition, Esco2 has been identified as a candidate regulator of meiosis by generating the transcripts with expression profiles similar to that of Stra8 (9,15). Despite numerous recent advances in the study of Esco2, its exact role during oocyte meiosis has still remained elusive.

In the current study, we document that Esco2 is required for proper spindle assembly, chromosome alignment and K-M attachment to ensure euploidy during mouse oocyte meiotic maturation. More importantly, we find that Esco2 is implicated in Spindle Assembly Checkpoint (SAC) activity by binding to histone H4 and regulating H4K16 acetylation. Our findings indicate that Esco2 exerts a novel function beyond its role in cohesion establishment via a different target during oocyte meiosis.

MATERIALS AND METHODS

Antibodies

Rabbit polyclonal anti-Esco2 antibody were purchased from Bethyl Laboratories (Cat#: A301-689A-T); mouse monoclonal anti-α-tubulin-FITC antibody was purchased from Sigma (Cat#: F2168, T7451 and T6557); human anti-centromere antibody was purchased from Antibod-

*To whom correspondence should be addressed. Tel: +86 25 8439 9605; Fax: +86 25 8439 9605; Email: xiongbo@njau.edu.cn

ies Incorporated (Cat#: CA95617); Rabbit polyclonal anti-histone H4 antibody and rabbit polyclonal anti-histone H4 (acetyl K16) antibody were purchased from Abcam (Cat#: ab177840, ab109463). Rabbit polyclonal anti-acetyl-histone H4 (Lys5) antibody was purchased from Cell Signaling Technology (Cat#: 9672).

Oocyte collection and culture

All experiments were approved by the Animal Care and Use Committee of Nanjing Agricultural University, China and were performed in accordance with institutional guidelines. Female ICR mice (4–6 weeks) were sacrificed by cervical dislocation after intraperitoneal injections of 5 IU PMSG for 46 h. GV oocytes were collected from ovaries in M2 medium (Sigma) and then cultured further in M16 medium (Sigma) under liquid paraffin oil at 37°C in an atmosphere of 5% CO2 incubator for *in vitro* maturation. At different time points after culture, oocytes were collected for subsequent analysis.

cRNA construct and *in vitro* transcription

Wild-type and mutant Esco2 or mutant H4 cDNA was sub-cloned into pcDNA3.1 vector, respectively. Capped cRNA was synthesized from linearized plasmid using T7 mMessage mMachine kit (ThermoFisher), and purified with MEGAclear kit (ThermoFisher). Typically, 10–12 pl of 0.5-1.0 μg/μl cRNA was injected into oocytes and then arrested at the GV stage in M16 medium containing 2.5 μM milrinone for 6 h, allowing enough time for translation, followed by releasing into milrinone-free M16 medium for further study.

Morpholino knockdown

Esco2-targeting morpholino (5′-TCTTGGAGTAC AAGTTGCCATCATC-3′) was obtained from Gene Tools LLC, and then diluted to 1mM as working concentration. For knockdown experiment, about 5–10 pl of morpholino was microinjected into the cytoplasm of GV oocytes. A non-targeting morpholino (5′-CCTCTTACCTCAGTTACAATTTATA-3′) was injected as a control. In order to facilitate the morpholino-mediated inhibition of mRNA translation, oocytes were arrested at GV stage in M16 medium containing 2.5 μM milrinone for 20 h and then cultured in milrinone-free M16 medium for subsequent experiments.

Immunofluorescence and confocal microscopy

Oocytes were fixed in 4% paraformaldehyde in PBS (pH 7.4) for 30 min and permeabilized in 0.5% Triton-X-100 for 20 min at room temperature. Then, oocytes were blocked with 1% BSA-supplemented PBS for 1 h and incubated with anti-Esco2 (1:50), anti-α-tubulin-FITC (1:300), anti-centromere (1:200) or anti-histone H4 (acetyl K16) (1:100) antibodies at 4°C overnight. After washing in Phosphate Buffered Saline with Tween-20 (PBST), oocytes were incubated with an appropriate secondary antibody for 1 h at room temperature. Then oocytes were counterstained with PI or Hoechst for 10 min. Finally, oocytes were mounted on glass slides and observed under a confocal microscope (Carl Zeiss 700).

For measurement of immunofluorescent intensity, the signals from both control and experimental oocytes were acquired by performing the same immunostaining procedure and setting up the same parameters of confocal microscope. Data were analyzed by Image J software.

Immunoprecipitation and immunoblotting analysis

Immunoprecipitation was carried out using 800 oocytes according to the Instructions for ProFound Mammalian Co-Immunoprecipitation Kit (ThermoFisher).

For immunoblotting, oocytes was lysed in 4 × Lithium Dodecyl Sulfate (LDS) sample buffer (ThermoFisher) containing protease inhibitor, and then separated on 10% Bis-Tris precast gels and transferred onto PVDF membranes. The blots were blocked in TBST containing 5% low fat dry milk for 1 h at room temperature and then incubated with anti-Esco2 (1:1000), anti-histone H4 (acetyl K16) (1:500), anti-histone-H4 (1:1000) or anti-Gapdh (1:5000) antibodies overnight at 4°C. After wash in TBST, the blots were incubated with HRP-conjugated secondary antibodies for 1 h at room temperature. Chemiluminescence was detected with ECL Plus (GE Healthcare) and protein bands were visualized by Tanon-3900.

In vitro acetylation assay

Full-length Esco2 and mutant Esco2-W530G cDNAs were sub-cloned into pcDNA3.1/Flag vector, respectively, and then transfected into HEK293 cells for expression, followed by flag purification. Recombinant histone H4 was purchased from NEB (Cat#: M2504S). For the *in vitro* acetylation assay, 1 μg of recombinant histone H4 was incubated with 250 ng of purified Esco2-Flag or Esco2-W530G-Flag in 50 μl of acetyltransferase assay buffer (50 mM Tris–HCl pH8.0, 10% glycerol, 10 mM butyric acid, 0.1 mM ethylenediaminetetraacetic acid, 1 mM Dithiothreitol (DTT) and 1mM Phenylmethylsulfonyl fluoride (PMSF) with or without 10 μM Ac-CoA (Sigma) at 30°C for 1 h on a rotating platform. The reaction was then stopped by adding sodium dodecyl sulphate-polyacrylamide gel electrophoresis loading buffer and analyzed by western blotting with anti-H4K16ac antibody.

Statistical analysis

All percentages from at least three repeated experiments were expressed as mean ± SEM, and the number of oocytes observed was labeled in parenthesesas (n). Data were analyzed by paired-samples *t*-test, which was provided by GraphPad Prism5 statistical software. The level of significance was accepted as $P < 0.05$.

RESULTS

Esco2 localizes to the chromosomes during mouse oocyte meiotic maturation

To examine the subcellular localization of Esco2 in various developmental stages during oocyte meiotic matura-

tion, immunofluorescent staining coupled with confocal microscopy was performed. The result showed that Esco2 appeared to accumulate on the chromosomes from GVBD (germinal vesicle breakdown) to metaphase II stages (Figure 1A). The close observation revealed that Esco2 predominantly distributed along the interstitial axes of chromosomes extending over centromere regions and arm regions both proximal and distal to chiasmata (Figure 1B). In addition, another pool of Esco2 was found in the periphery of sisters of homologs (Figure 1B). The chromosome arm localization pattern of Esco2 is consistent with the cohesin subunits such as Rec8 (16), but the periphery localization pattern indicates that Esco2 might have a unique function other than that in chromosome cohesion process.

In HeLa cells, Esco2 is absent in mitosis and reappears when the cells enter S phase of the next cell cycle (17). Inconsistent with this expression pattern, we showed that the protein level of Esco2 in oocyte meiosis was increasingly upregulated from prophase I to metaphase II stages (Figure 1C), which suggests that the role of Esco2 is not restricted to S phase in germ cells.

Esco2 is required for meiotic progression and activation of SAC during oocyte meiosis

To clearly investigate the functional roles of Esco2 in oocytes, loss-of-function experiments via gene-targeting morpholino microinjection were carried out to deplete Esco2 in oocytes. A significant decrease of Esco2 protein level was shown in Esco2-depleted oocytes compared to controls by both western blot and immunofluorescence analysis (Figure 2A and Supplementary Figure S1), suggesting that Esco2 was successfully depleted by morpholino-based silencing approach. To test if Esco2 is required for the meiotic progression, GVBD and PBE (polar body extrusion), two critical developmental events during oocyte maturation, were examined after knockdown. The quantitative results showed that there were no distinguishable differences of GVBD rate between Esco2-depleted oocytes and controls (71.78 ± 1.97%, $n = 209$ versus 76.78 ± 2.35%, $n = 222$ control; Figure 2B). However, at the time point of 6, 7 and 8 h post-GVBD, a significantly higher incidence of PBE was observed in Esco2-depleted oocytes than that in control oocytes (6.23 ± 0.85%, $n = 129$ versus 0.67 ± 0.67%, $n = 138$ control, $P < 0.05$; 27.18 ± 3.45%, $n = 129$ versus 12.18 ± 1.26%, $n = 138$ control, $P < 0.05$; 50.52 ± 3.83%, $n = 129$ versus 30.77 ± 3.40%, $n = 138$ control, $P < 0.05$; Figure 2C and D), suggesting that meiotic progression was accelerated and SAC was inactivated in the absence of Esco2. To rule out the possibility that premature PBE we observed was due to the off-target effects of morpholino, we expressed the exogenous Esco2 by injecting its cRNA in Esco2-depleted oocytes to monitor the meiotic progression. As expected, in the rescue oocytes, the rates of PBE at the time point of 6, 7 and 8 h post-GVBD were decreased to the control comparable levels (2.14 ± 0.01%, $n = 140$; 14.97 ± 2.05%, $n = 140$; 33.52 ± 4.15%, $n = 140$; Figure 2C and D).

To further confirm the SAC control by Esco2, we tested whether oocytes depleted of Esco2 would override the metaphase I arrest induced by nocodazole treatment, indicative of SAC inactivation. The result showed that only

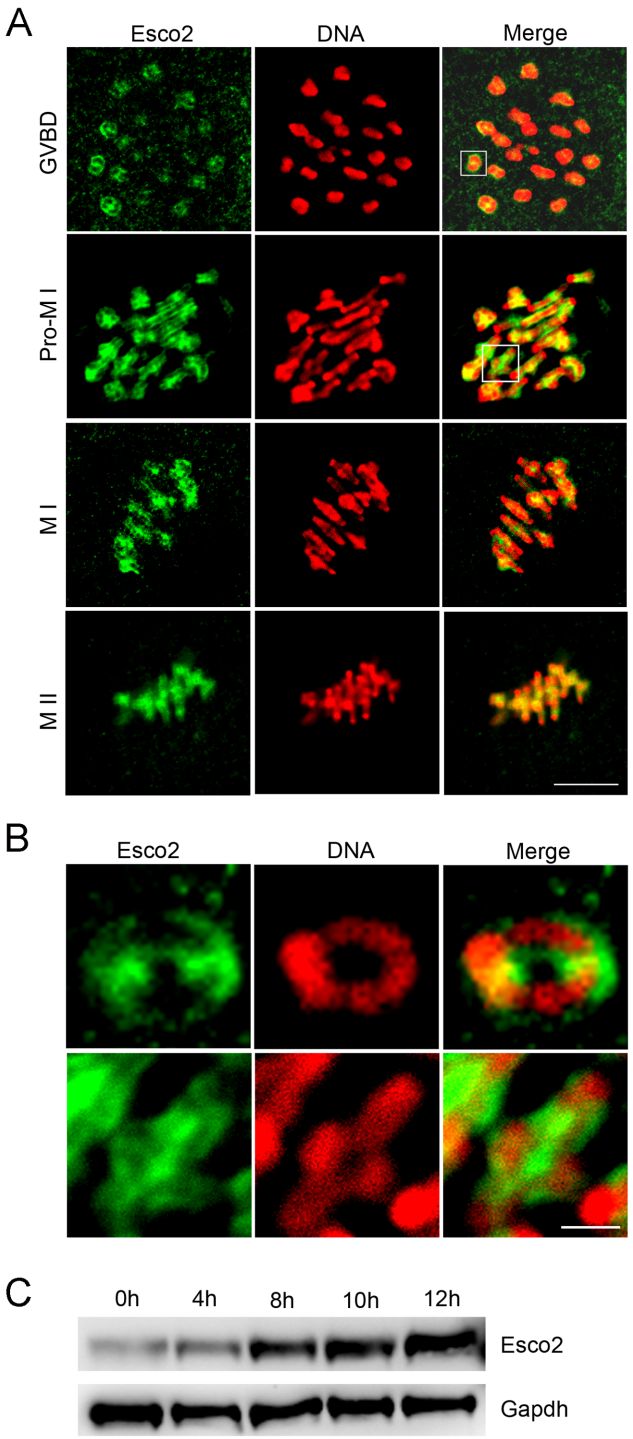

Figure 1. Subcellular localization and expression of Esco2 during mouse meiotic maturation. (**A**) Mouse oocytes at GVBD, prometaphase I, metaphase I and metaphase II stages were immunolabeled with anti-Esco2 antibody and counterstained with PI. Scale bar, 2.5 μm. (**B**) The magnified images from panel A. Scale bar, 0.5 μm. (**C**) Protein levels of Esco2 in oocytes corresponding to GV (0 h), GVBD (4 h), MI (8 h), ATI (10 h) and MII (12 h) stages were examined by western blot.

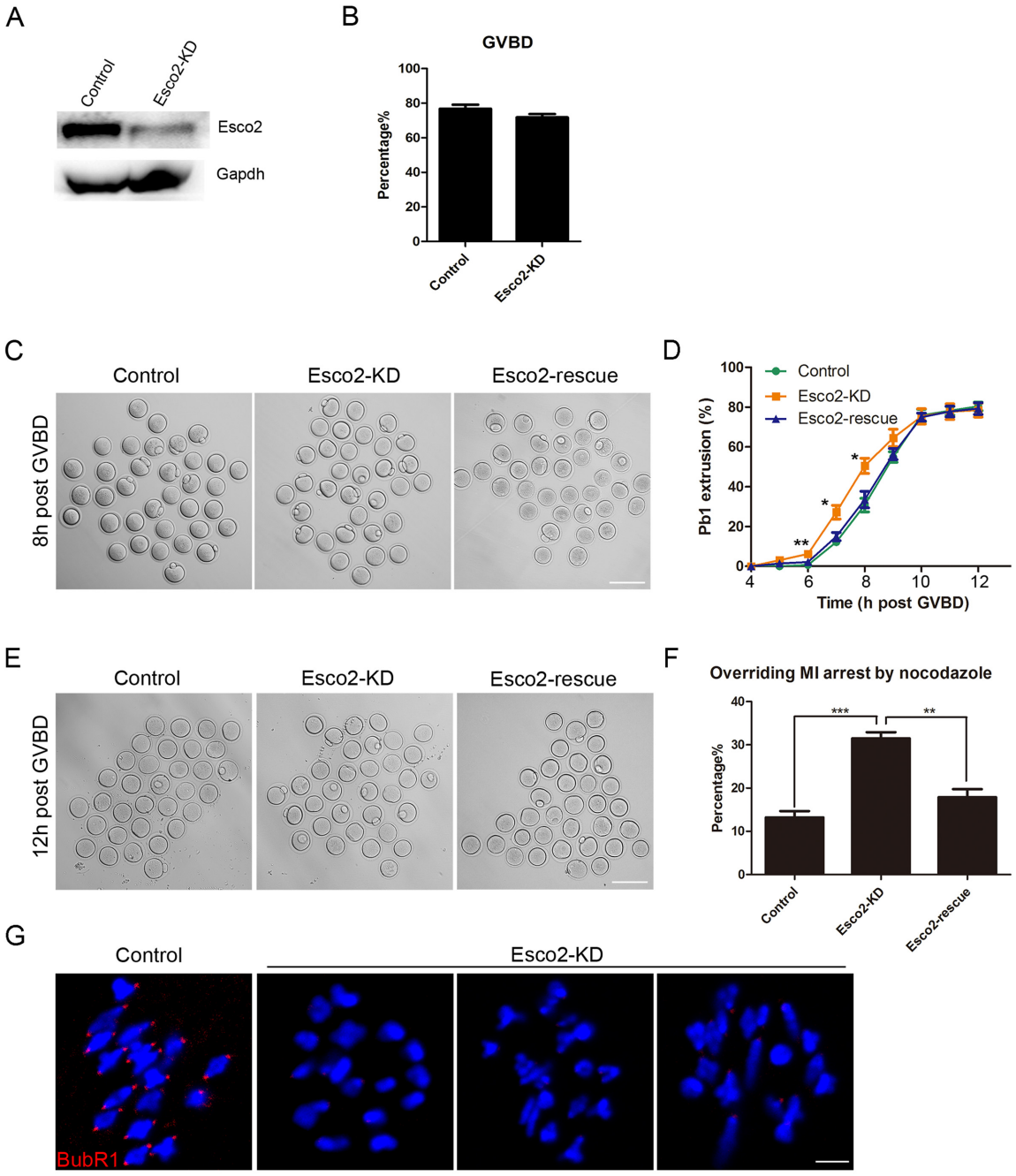

Figure 2. Effects of Esco2 depletion on the meiotic progression and SAC activity in mouse oocytes. (**A**) Protein levels of Esco2 in control and Esco2-KD oocytes at M I stage were examined by western blot. (**B**) Quantitative analysis of GVBD rate was shown in control and Esco2-KD oocytes. (**C**) Representative images of first polar body extrusion(PBE) in control, Esco2-KD and Esco2-rescue oocytes at the time point of 8 h post-GVBD. Scale bar, 200 μm. (**D**) Quantitative analysis of PBE rate was shown in control, Esco2-KD and Esco2-rescue oocytes at consecutive time points of post-GVBD. (**E**) Representative images of first PBE in control, Esco2-KD and Esco2-rescue oocytes treated with low dose of nocodazole. Scale bar, 200 μm. (**F**) The proportion of overriding M I arrest was recorded in control, Esco2-KD and Esco2-rescue oocytes. (**G**) Localization of BubR1 at prometaphase I stage in control and Esco2-KD oocytes. Scale bar, 2.5 μm. Data of (B), (D) and (F) were presented as mean percentage (mean ± SEM) of at least three independent experiments. Asterisk denotes statistical difference at a $P < 0.05$ level of significance.

about 13% of control oocytes could abrogate MI arrest and extrude the first polar body (Figure 2E and F). However, Esco2-depleted oocytes displayed a remarkably increased overriding incidence and around 31% of oocytes escaped the MI arrest to reach the MII stage (31.49 ± 1.44%, n = 101 versus 13.23 ± 1.47%, n = 99 control, $P < 0.05$; Figure 2E and F). In the meantime, this increased rate of MI escape in Esco2-depleted oocytes could be rescued to the control indistinguishable level by expressing the exogenous Esco2 (17.88 ± 1.87%, n = 95 rescue; Figure 2E and F).

Finally, we examined the SAC activity by immunostaining BubR1, an integral part of SAC complex, and its absence causes the loss of SAC control (18). As shown in Figure 2G, BubR1 was localized to the unattached kinetochores at prometaphase I stage in control oocytes. However, BubR1 was lost from most of kinetochores in Esco2-depleted oocytes, indicating that Esco2 depletion impairs the SAC complex and activity.

Taken together, the above results indicate that Esco2 is implicated in the activation of SAC during meiotic progression.

Esco2 is necessary for spindle assembly and chromosome alignment during oocyte meiosis

We next examined the spindle assembly and chromosome alignment in Esco2-depleted oocytes. To this end, mouse oocytes from control and Esco2-depleted groups were immunolabeled with anti-α-tubulin antibody to visualize the spindle morphologies and counterstained with PI to observe the chromosome alignment. We found a significant increased percentage of spindle defects (76.60 ± 4.51%, n = 94 versus 18.97 ± 1.83%, n = 95 control, $P < 0.05$; Figure 3A and B) and chromosome misalignment (76.67 ± 2.46%, n = 94 versus 23.11 ± 1.69%, n = 95 control, $P <$ 0.05; Figure 3A and C) in Esco2-depleted oocytes, exhibiting diverse malformed spindle morphologies with several scattered or lagging chromosomes (Figure 3A). By striking contrast, control oocytes at M I stage usually show a typical barrel-shape spindle and well-aligned chromosomes at the equator (Figure 3A). In addition, we measured the width of chromosome plate at M I stage and found it remarkably wider in Esco2-depleted oocytes than the controls (23.46 ± 0.51%, n = 94 versus 13.01 ± 0.39%, n = 95 control, $P <$ 0.05; Figure 3D). Consistent with the defective M I spindle assembly, M II spindles also displayed a substantially higher rate of abnormality after Esco2 depletion (74.44 ± 4.84%, n = 90 versus 21.11 ± 2.94%, n = 84 control, $P <$ 0.05; Supplementary Figure S2).

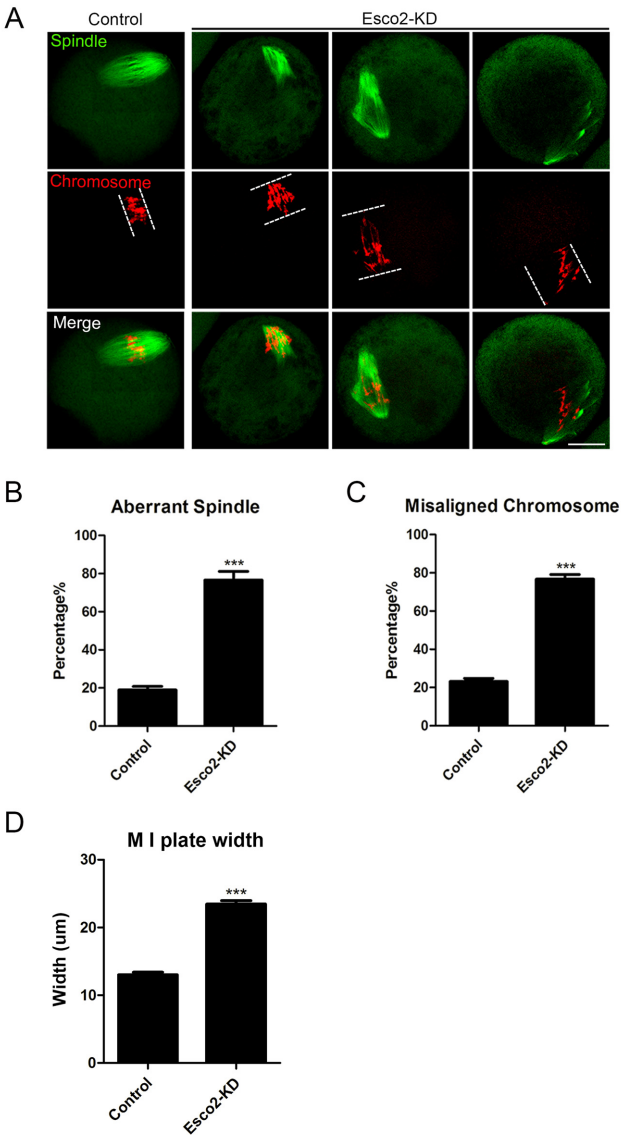

Figure 3. Depletion of Esco2 causes spindle/chromosome abnormalities in mouse oocytes. (**A**) Representative images of spindle morphologies and chromosome alignment in control and Esco2-KD oocytes. Scale bar, 20 μm. (**B**) The proportion of abnormal spindles was recorded in control and Esco2-KD oocytes. (**C**) The proportion of misaligned chromosomes was recorded in control and Esco2-KD oocytes. (**D**) The width of M I plate was measured in control and Esco2-KD oocytes. Data of (B–D) were presented as mean percentage (mean ± SEM) of at least three independent experiments. Asterisk denotes statistical difference at a $P < 0.05$ level of significance.

Esco2 maintains the stability of K-MT attachments and prevents the incidence of aneuploidy in oocytes

The high percentage of spindle/chromosome abnormalities predicts the compromised K-MT attachments in Esco2-depleted oocytes. To test it, oocytes were exposed to cold treatment for inducing depolymerization of microtubules that are not attached to kinetochores and then immunolabeled with CREST to show kinetochores, with anti-α-tubulin-FITC antibody to visualize microtubule fibers and counterstained with Hoechst to observe chromosomes as described previously (19). We observed a prominently elevated frequency of kinetochores with very few cold-stable microtubules in Esco2-depleted oocytes (Figure 4A). By performing quantitative analysis, it was shown that depletion of Esco2 substantially increased the proportion of impaired K-MT attachments compared to control oocytes to 78 from 29% (78.59 ± 1.81%, n = 70 versus 29.44 ± 2.42%, n = 64 control, $P < 0.05$; Figure 4B). These K-MT attachment errors would inevitably result in the establishment of unstable chromosome biorientation, which is consistent

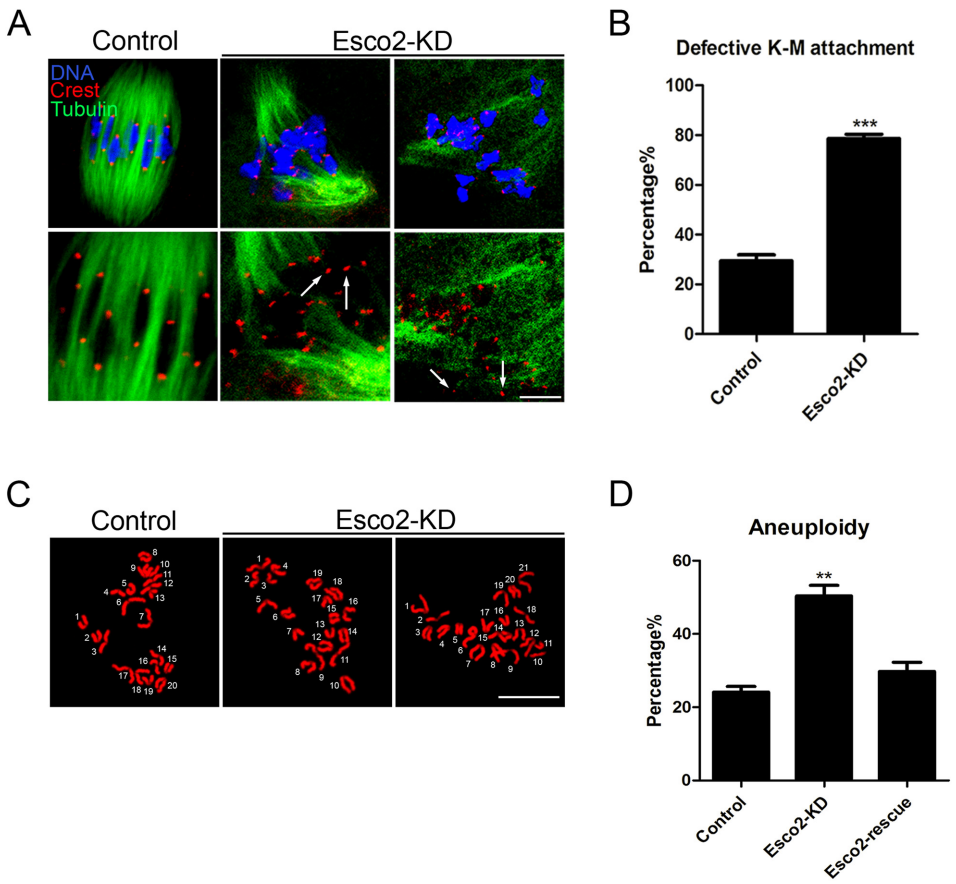

Figure 4. Depletion of Esco2 compromises K-M attachments and generates aneuploidy in mouse oocytes. (**A**) Representative images of kinetochore-microtubule attachments in control and Esco2-KD oocytes. Oocytes were immunostained with anti-α-tubulin-FITC antibody to visualize spindles, with CREST to visualize kinetochores and counterstained with Hoechst to visualize chromosomes. Scale bar, 5 μm. (**B**) The rate of defective kinetochore-microtubule attachments was recorded in control and Esco2-KD oocytes. (**C**) Representative images of euploid and aneuploid MII eggs. Chromosome spread was performed to count the number of chromosomes in control and Esco2-KD oocytes. Chromosomes were counterstained with Hoechst. Scale bar, 2.5 μm. (**D**) The rate of aneuploid eggs was recorded in control and Esco2-KD oocytes. Data of (B and D) were presented as mean percentage (mean ± SEM) of at least three independent experiments. Asterisk denotes statistical difference at a $P < 0.05$ level of significance.

with the above observation of aneuploidy in the absence of Esco2.

To ask if the loss of Esco2 would generate aneuploidy in oocytes, karyotypic analysis of MII eggs was performed by chromosome spreading. We found that a large proportion of control oocytes had correct number of univalents to maintain the euploidy (Figure 4C). However, the incidence of aneuploid eggs that had more or less 20 univalents in Esco2-depleted oocytes increased about two fold compared to that in controls (50.37 ± 2.92%, $n = 49$ versus 24.13 ± 1.56%, $n = 50$ control, $P < 0.05$, Figure 4D), suggesting that Esco2 is required to protect oocytes from aneuploidy. Consistently, in the rescue oocytes, the rate of aneuploidy was reduced to the normal level that was comparable to controls (29.78 ± 2.48%, $n = 37$; Figure 4D). Therefore, these observations reveal that loss of Esco2 inactivates SAC in oocytes, consequently generating aneuploid eggs.

Esco2 binds to histone H4 and is required for maintaining the acetylation status of H4K16 in oocytes

The involvement of Esco2 in activation of SAC and kinetochore functions prompted us to further explore the underlying mechanisms. On the other hand, it has been recently reported that H4K16 acetylation plays an important role in establishment of functional kinetochore in mouse oocytes (20,21), we thus hypothesized that Esco2 might participate in the SAC and kinetochore functions by maintaining the status of H4K16 acetylation during oocyte meiosis. To verify this possibility, we first examined the acetylation level of H4K16 by immunostaining analysis. The quantitative result of fluorescence intensity showed that signals of H4K16 acetylation were remarkably reduced in Esco2-depleted oocytes in comparison with controls (17.32 ± 2.07, $n = 51$ versus 35.30 ± 3.31, $n = 51$ control, $P < 0.05$; Figure 5A and B), but restored to the level indistinguishable from controls following the expression of exogenous Esco2 cRNA (30.04 ± 3.22, $n = 45$; Figure 5A and B). However, the acetylation level of H4K16 could not be restored in Esco2-depleted oocytes exogenously expressing Esco2-W530G mutant cRNA (16.71 ± 2.23, $n = 42$; Figure 5A and B), which corresponds to its conserved mutation Esco2-W539G in human cells that has been found to result in

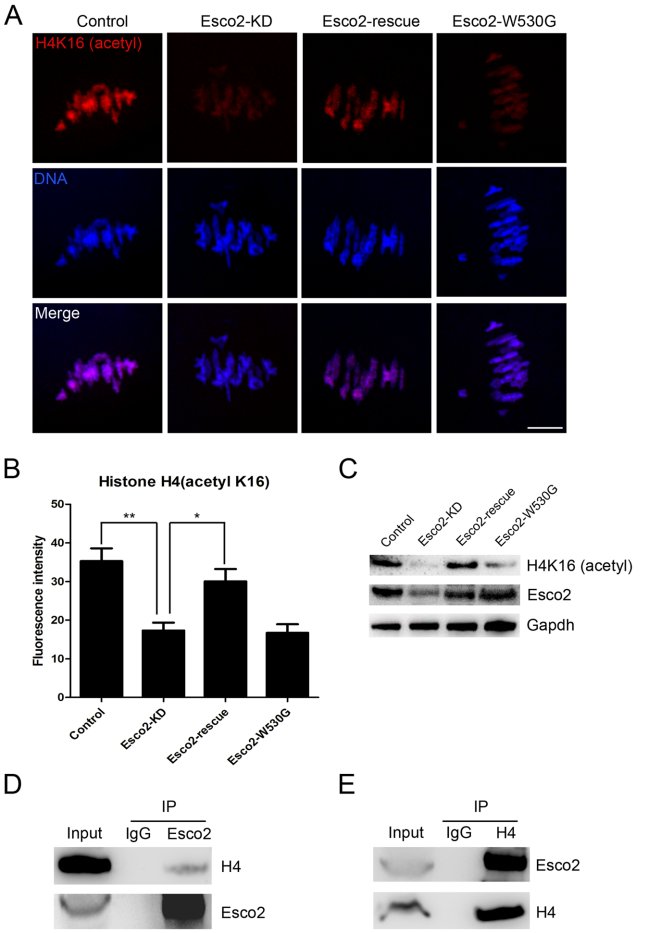

Figure 5. Esco2 binds to histone H4 to regulate the acetylation level of H4K16. (**A**) Representative images of acetylated H4K16 in control, Esco2-KD, Esco2-rescue and Esco2-W530G oocytes. Scale bar, 5 μm. (**B**) The immunofluorescence intensity of acetylated H4K16 was recorded in control, Esco2-KD, Esco2-rescue and Esco2-W530G oocytes. Data were presented as mean percentage (mean ± SEM) of at least three independent experiments. Asterisk denotes statistical difference at a $P < 0.05$ level of significance. (**C**) Acetylation levels of H4K16 in control, Esco2-KD, Esco2-rescue and Esco2-W530G oocytes were examined by western blotting. (**D**) IP was performed with the Esco2 antibody, and the blots of IP eluate were probed with anti-Esco2 and anti-histone H4 antibodies, respectively. (**E**) IP was performed with the histone H4 antibody, and the blots of IP eluate were probed with anti-Esco2 and anti-histone H4 antibodies, respectively.

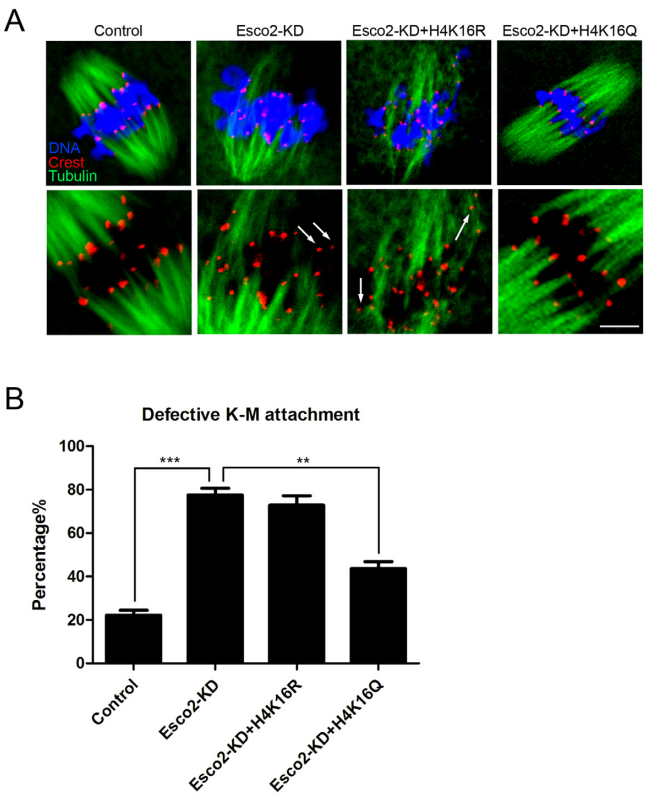

Figure 6. H4K16Q rescues the defect of K-M attachments in Esco2-depleted oocytes. (**A**) Representative images of kinetochore-microtubule attachments in control, Esco2-KD, Esco2-KD+H4K16R and Esco2-KD+H4K16Q oocytes. Scale bar, 5 μm. (**B**) The rate of defective kinetochore-microtubule attachments was recorded in control, Esco2-KD, Esco2-KD+H4K16R and Esco2-KD+H4K16Q oocytes. Data were presented as mean percentage (mean ± SEM) of at least three independent experiments. Asterisk denotes statistical difference at a $P < 0.05$ level of significance.

loss of acetyltransferase activity (22,23). These observations were further confirmed by the western blotting analysis (Figure 5C), implying that H4K16 is the potential substrate of Esco2 in oocytes. We also detected the acetylation level of H4K5 by western blotting and found it unaffected in Esco2-depleted oocytes, suggesting that Esco2 specifically targets H4K16 (Supplementary Figure S3). Moreover, we carried out Co-IP to determine the interaction between Esco2 and histone H4. Immunoprecipitation was first performed with Esco2 antibody. The blot of IP eluate probed by Esco2 antibody showed that Esco2 was specifically present in the antibody group instead of IgG control group (Figure 5D), suggesting that the complex containing Esco2 was pulled down in the eluate. Meanwhile, the blot probed by H4 antibody also showed the exclusive presence of H4 in the antibody group (Figure 5D). Reciprocally, Esco2 was specifically present in the IP eluate which was pulled down by H4 antibody (Figure 5E), indicating that Esco2 associates with H4 in oocytes. Additionally, we tested whether acetylation status of H4K16 would affect the kinetochore-microtubule attachments in Esco2-depleted oocytes. The result showed that H4K16Q acetylmimic mutation but not H4K16R non-acetylatable mutation restored the impaired the kinetochore-microtubule attachments in the Esco2-depleted oocytes (Control: 22.22 ± 2.22% $n = 45$, Esco2-KD: 77.56 ± 3.09% $n = 40$, Esco2-KD + H4K16R: 72.84 ± 4.36% $n = 48$, Esco2-KD + H4K16Q: 43.73 ± 3.16% $n = 50$; Figure 6A and B). Collectively, the alteration of H4K16 acetylation in Esco2-depleted oocytes may perturb the chromatin conformation and kinetochore function, contributing, at least in part, to the spindle defects, chromosome misalignment and SAC activity during meiosis. Certainly we cannot rule out the possibility that Esco2 acts on other targets in this process. Future investigations will be required to uncover these details.

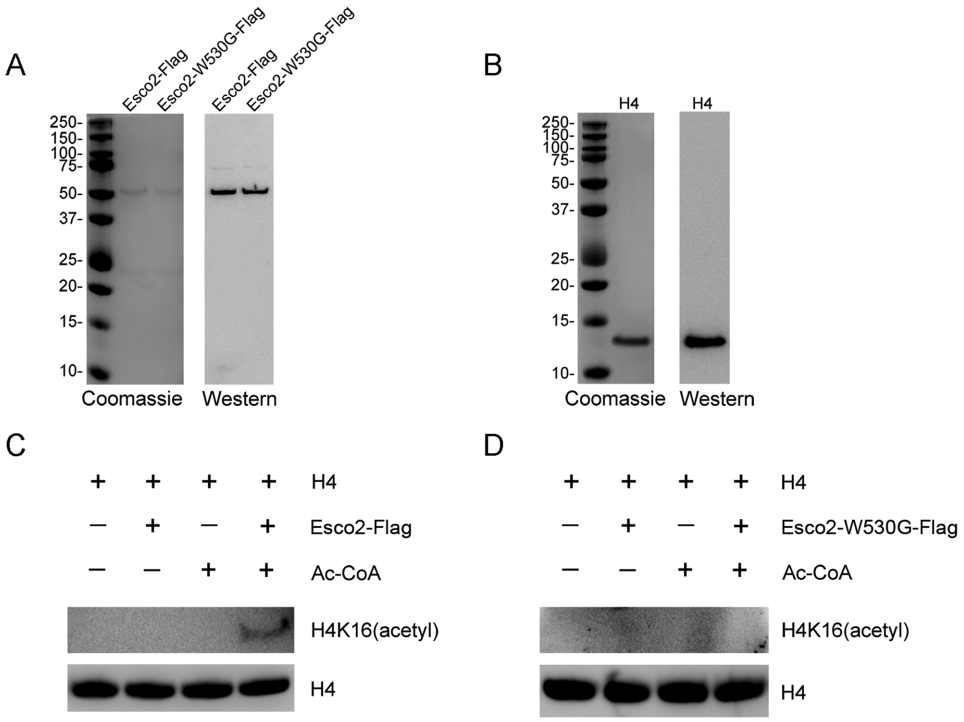

Figure 7. Esco2 acetylates histone H4 at Lys16 *in vitro*. (**A**) Flag purification of Esco2. Esco2 and enzymatically mutant Esco2-W530G were expressed in HEK293 cells and then purified according to the Flag purification procedure. Purified Esco2-Flag and Esco2-W530G-Flag were detected with sodium dodecyl sulphate-polyacrylamide gel electrophoresis followed by both coomassie staining and western blotting with anti-Esco2 antibody. (**B**) Commercially obtained recombinant histone H4 was identified by both coomassie staining and western blotting with anti-H4 antibody. (**C**) *In vitro* acetylation assay with Esco2-Flag. Recombinant histone H4 was incubated with or without purified Esco2-Flag and Ac-CoA in the acetyltransferase assay buffer at 30°C for 1 h. The reactions were analyzed by western blotting with anti-histone H4 (acetyl K16) antibody for acetylation levels of H4K16 and anti-histone H4 antibody as a loading control. (**D**) *In vitro* acetylation assay with Esco2-W530G-Flag. Recombinant histone H4 was incubated with or without purified Esco2-W530G-Flag and Ac-CoA in the acetyltransferase assay buffer at 30°C for 1 h. The reactions were analyzed by western blotting with anti-histone H4 (acetyl K16) antibody for acetylation levels of H4K16 and anti-histone H4 antibody as a loading control.

Esco2 acetylates histone H4 at Lys16 *in vitro*

To determine whether Esco2 can directly acetylate H4 at Lys16, both Esco2-Flag and enzymatically dead Esco2-W530G-Flag were purified from HEK293 cells by flag purification. In the coomassie stained gel, the bands in Esco2-Flag and Esco2-W530G-Flag lanes were specifically present in the same position which were further confirmed by western blotting with anti-Esco2 antibody (Figure 7A). Recombinant histone H4 was purified from E. coli and also identified by coomassie staining and western blotting analysis (Figure 7B).

We next performed *in vitro* acetylation assay using the purified proteins. We found that recombinant histone H4 was acetylated at Lys16 in the presence of both Esco2-Flag and Ac-CoA in an *in vitro* assay system (Figure 7C). By contrast, under the same conditions Esco2-W530G-Flag had no acetyltransferase activity toward the recombinant histone H4 (Figure 7D). Thus, this observation provides the direct evidence that Esco2 targets histone H4 at Lys16.

DISCUSSION

The well-known role of Esco2 is mediating the acetylation of cohesin subunit Smc3 to establish the chromosome cohesion in S phase, ensuring the proper chromosome segregation to maintain the genome stability. In mammalian females, chromosome cohesion is established when meiotic DNA replication and recombination occur in fetal oocytes. After birth, oocytes arrest at the prolonged prophase I stage until recruited to grow into mature oocytes that divide at ovulation, but bivalent cohesion is maintained without detectable turnover (24,25). Thus, during the developmental window of oocyte meiotic maturation, chromosome cohesion does not require Esco2 to exert any function as the establishment factor. Because of the nature of acetyltransferase, Esco2 must have several unknown substrates that function in other biological processes. In the present study, we have determined a distinctive role of Esco2 during mouse oocyte meiotic maturation instead of a cohesion establishment factor.

Eco1 in budding yeast localizes to chromosomes throughout the cell cycle (26). In both HeLa cells and 293T cells, ∼70% of the endogenous Esco2 associates with chromosomes and the rest are found in the soluble fractions that are contributed by the cytoplasmic Esco2 fractions (17). During meiosis Esco2 is reported to localize to the XY body in spermatocytes and accumulate to chromatin regions containing double-stranded breaks in the embryonic ovary (27). Our findings showed that Esco2 has two pools of localization patterns on the chromosomes during oocyte meiotic maturation. The localization along the interstitial axes of chromosomes is the same as the

cohesin subunits. The periphery of sisters of homologs localization which covers the region that the kinetochore localizes at the chromosome indicates that Esco2 might be involved in other biological events such as the regulation of kinetochore functions. In addition, the protein expression of Esco2 during oocyte meiosis is different from that in mitosis. Esco2 degrades in the remainder of cell cycle after S phase in mitotic cells (17). However, we found that the protein level of Esco2 increases from prophase I to metaphase II stages in mouse oocytes, which predicts that the Esco2 has the additional functions beyond S phase during oocyte meiosis.

To ask whether Esco2 has a distinctive role during oocyte maturation, we depleted Esco2 by the morpholino-based gene silencing in oocytes. We found that Esco2 is not indispensable for the meiotic progression but is required for SAC activation as depletion of Esco2 caused the premature PBE, the escape of M I arrest induced by nocodazole and the loss of BubR1 from kinetochores. These observations are in line with the previous studies in mouse oocytes that loss of SAC components leads to the strong acceleration of meiosis I and severe chromosome missegregations (18,28,29). Also, compared with mitosis, SAC is not very efficient in meiosis, and the presence of one or few incorrectly attached kinetochores with reduced K-MT tension escapes checkpoint detection in mouse oocytes (30–32). Since SAC inactivation is usually accompanied by the defects of spindle/chromosome abnormalities, we thus examined the spindle assembly and chromosome alignment in the absence of Esco2. The findings revealed that Esco2 plays a critical role in the maintenance of normal spindle formation, chromosome alignment and kinetochore-microtubule attachment, thereby ensuring euploidy during oocyte meiosis. It has been reported that SAC activity is dependent on the cohesin in the oocyte but not in zygote, suggesting that this dependence is a feature specific to the oocyte (33,34). Our data further demonstrates that cohesin regulator Esco2 is also involved in the regulation of SAC in the oocyte. Then another question is raised: what is the downstream effector of Esco2 that mediates this process? Because acetylation of H4K16 has been shown to participate in the establishment of functional kinetochores in mouse oocytes (20,21), we then tested whether Esco2 acts as a SAC regulator via maintaining the acetylation level of H4K16. Our findings manifested that Esco2 associates with histone H4 and is required for H4K16 acetylation. WT but not catalytically dead mutation of Esco2 could rescue the reduced acetylation level of H4K16 in depletion of Esco2. Also, H4K16Q acetylmimic mutation but not H4K16R non-acetylatable mutation restored the compromised the kinetochore-microtubule attachment in the Esco2-depleted oocytes. More importantly, we performed the *in vitro* acetylation assay using the purified proteins to show that Esco2 can directly acetylate histone H4 at Lys16. Therefore, we demonstrate that Esco2 maintains the acetylation status of H4K16 to take part in the kinetochore functions.

Collectively, we provide a body of evidence that Esco2 plays an important role in the kinetochore functions for SAC activity to ensure the euploidy via binding to histone H4 to regulate H4K16 acetylation status in mouse oocytes. These observations uncover a novel meiotic function to Esco2 beyond its role in chromosome cohesion.

SUPPLEMENTARY DATA

Supplementary Data are available at NAR Online.

ACKNOWLEDGEMENTS

We thank Dr Shaochen Sun for extensive advice and constructive comments on the manuscript.

FUNDING

National Natural Science Foundation of China [31571545]; Natural Science Foundation of Jiangsu Province [BK20150677]. Funding for open access charge: National Natural Science Foundation of China [31571545].
Conflict of interest statement. None declared.

REFERENCES

1. Xiong,B. and Gerton,J.L. (2010) Regulators of the cohesin network. *Annu. Rev. Biochem.*, **79**, 131–153.
2. Onn,I., Heidinger-Pauli,J.M., Guacci,V., Unal,E. and Koshland,D.E. (2008) Sister chromatid cohesion: a simple concept with a complex reality. *Annu. Rev. Cell Dev. Biol.*, **24**, 105–129.
3. Nasmyth,K. and Haering,C.H. (2009) Cohesin: its roles and mechanisms. *Annu. Rev. Genet.*, **43**, 525–558.
4. Saito,Y., Zhou,H. and Kobayashi,J. (2016) Chromatin modification and NBS1: their relationship in DNA double-strand break repair. *Genes Genet. Syst.*, **90**, 195–208.
5. Rolef Ben-Shahar,T., Heeger,S., Lehane,C., East,P., Flynn,H., Skehel,M. and Uhlmann,F. (2008) Eco1-dependent cohesin acetylation during establishment of sister chromatid cohesion. *Science*, **321**, 563–566.
6. Unal,E., Heidinger-Pauli,J.M., Kim,W., Guacci,V., Onn,I., Gygi,S.P. and Koshland,D.E. (2008) A molecular determinant for the establishment of sister chromatid cohesion. *Science*, **321**, 566–569.
7. Rowland,B.D., Roig,M.B., Nishino,T., Kurze,A., Uluocak,P., Mishra,A., Beckouet,F., Underwood,P., Metson,J., Imre,R. *et al.* (2009) Building sister chromatid cohesion: smc3 acetylation counteracts an antiestablishment activity. *Mol. Cell*, **33**, 763–774.
8. Sutani,T., Kawaguchi,T., Kanno,R., Itoh,T. and Shirahige,K. (2009) Budding yeast Wpl1(Rad61)-Pds5 complex counteracts sister chromatid cohesion-establishing reaction. *Curr. Biol.*, **19**, 492–497.
9. Vega,H., Waisfisz,Q., Gordillo,M., Sakai,N., Yanagihara,I., Yamada,M., van Gosliga,D., Kayserili,H., Xu,C., Ozono,K. *et al.* (2005) Roberts syndrome is caused by mutations in ESCO2, a human homolog of yeast ECO1 that is essential for the establishment of sister chromatid cohesion. *Nat. Genet.*, **37**, 468–470.
10. Cao,Q., Wang,Y., Chen,F., Xia,Y., Lou,J., Zhang,X., Yang,N., Sun,X., Zhang,Q., Zhuo,C. *et al.* (2014) A novel signal transduction pathway that modulates rhl quorum sensing and bacterial virulence in Pseudomonas aeruginosa. *PLoS Pathog.*, **10**, e1004340.
11. Whelan,G., Kreidl,E., Peters,J.M. and Eichele,G. (2012) The non-redundant function of cohesin acetyltransferase Esco2: some answers and new questions. *Nucleus*, **3**, 330–334.
12. Nishiyama,T., Ladurner,R., Schmitz,J., Kreidl,E., Schleiffer,A., Bhaskara,V., Bando,M., Shirahige,K., Hyman,A.A., Mechtler,K. *et al.* (2010) Sororin mediates sister chromatid cohesion by antagonizing Wapl. *Cell*, **143**, 737–749.
13. Goh,E.S., Li,C., Horsburgh,S., Kasai,Y., Kolomietz,E. and Morel,C.F. (2010) The Roberts syndrome/SC phocomelia spectrum–a case report of an adult with review of the literature. *Am. J. Med. Genet. A*, **152**, 472–478.
14. Whelan,G., Kreidl,E., Wutz,G., Egner,A., Peters,J.M. and Eichele,G. (2012) Cohesin acetyltransferase Esco2 is a cell viability factor and is required for cohesion in pericentric heterochromatin. *EMBO J.*, **31**, 71–82.

15. Hogarth,C.A., Mitchell,D., Evanoff,R., Small,C. and Griswold,M. (2011) Identification and expression of potential regulators of the mammalian mitotic-to-meiotic transition. *Biol. Reprod.*, **84**, 34–42.
16. Rong,M., Matsuda,A., Hiraoka,Y. and Lee,J. (2016) Meiotic cohesin subunits RAD21L and REC8 are positioned at distinct regions between lateral elements and transverse filaments in the synaptonemal complex of mouse spermatocytes. *J. Reprod. Dev.*, **62**, 623–630.
17. Hou,F. and Zou,H. (2005) Two human orthologues of Eco1/Ctf7 acetyltransferases are both required for proper sister-chromatid cohesion. *Mol. Biol. Cell*, **16**, 3908–3918.
18. Touati,S.A., Buffin,E., Cladiere,D., Hached,K., Rachez,C., van Deursen,J.M. and Wassmann,K. (2015) Mouse oocytes depend on BubR1 for proper chromosome segregation but not for prophase I arrest. *Nat. Commun.*, **6**, 6946–6958.
19. Ma,R., Hou,X., Zhang,L., Sun,S.C., Schedl,T., Moley,K. and Wang,Q. (2014) Rab5a is required for spindle length control and kinetochore-microtubule attachment during meiosis in oocytes. *FASEB J.*, **28**, 4026–4035.
20. Choy,J.S., Acuna,R., Au,W.C. and Basrai,M.A. (2011) A role for histone H4K16 hypoacetylation in Saccharomyces cerevisiae kinetochore function. *Genetics*, **189**, 11–21.
21. Ma,P. and Schultz,R.M. (2013) Histone deacetylase 2 (HDAC2) regulates chromosome segregation and kinetochore function via H4K16 deacetylation during oocyte maturation in mouse. *PLoS Genet.*, **9**, e1003377.
22. van der Lelij,P., Godthelp,B.C., van Zon,W., van Gosliga,D., Oostra,A.B., Steltenpool,J., de Groot,J., Scheper,R.J., Wolthuis,R.M., Waisfisz,Q. *et al.* (2009) The cellular phenotype of Roberts syndrome fibroblasts as revealed by ectopic expression of ESCO2. *PLoS One*, **4**, e6936.
23. Gordillo,M., Vega,H., Trainer,A.H., Hou,F., Sakai,N., Luque,R., Kayserili,H., Basaran,S., Skovby,F., Hennekam,R.C. *et al.* (2008) The molecular mechanism underlying Roberts syndrome involves loss of ESCO2 acetyltransferase activity. *Hum. Mol. Genet.*, **17**, 2172–2180.
24. Burkhardt,S., Borsos,M., Szydlowska,A., Godwin,J., Williams,S.A., Cohen,P.E., Hirota,T., Saitou,M. and Tachibana-Konwalski,K. (2016) Chromosome cohesion established by Rec8-cohesin in fetal oocytes is maintained without detectable turnover in oocytes arrested for months in mice. *Curr. Biol.*, **26**, 678–685.
25. Tachibana-Konwalski,K., Godwin,J., van der Weyden,L., Champion,L., Kudo,N.R., Adams,D.J. and Nasmyth,K. (2010) Rec8-containing cohesin maintains bivalents without turnover during the growing phase of mouse oocytes. *Genes Dev.*, **24**, 2505–2516.
26. Toth,A., Ciosk,R., Uhlmann,F., Galova,M., Schleiffer,A. and Nasmyth,K. (1999) Yeast cohesin complex requires a conserved protein, Eco1p(Ctf7), to establish cohesion between sister chromatids during DNA replication. *Genes Dev.*, **13**, 320–333.
27. Evans,E.B., Hogarth,C., Evanoff,R.M., Mitchell,D., Small,C. and Griswold,M.D. (2012) Localization and regulation of murine Esco2 during male and female meiosis. *Biol. Reprod.*, **87**, 61–68.
28. Hached,K., Xie,S.Z., Buffin,E., Cladiere,D., Rachez,C., Sacras,M., Sorger,P.K. and Wassmann,K. (2011) Mps1 at kinetochores is essential for female mouse meiosis I. *Development*, **138**, 2261–2271.
29. McGuinness,B.E., Anger,M., Kouznetsova,A., Gil-Bernabe,A.M., Helmhart,W., Kudo,N.R., Wuensche,A., Taylor,S., Hoog,C., Novak,B. *et al.* (2009) Regulation of APC/C activity in oocytes by a Bub1-dependent spindle assembly checkpoint. *Curr. Biol.*, **19**, 369–380.
30. Nagaoka,S.I., Hodges,C.A., Albertini,D.F. and Hunt,P.A. (2011) Oocyte-specific differences in cell-cycle control create an innate susceptibility to meiotic errors. *Curr. Biol.*, **21**, 651–657.
31. Lane,S.I., Yun,Y. and Jones,K.T. (2012) Timing of anaphase-promoting complex activation in mouse oocytes is predicted by microtubule-kinetochore attachment but not by bivalent alignment or tension. *Development*, **139**, 1947–1955.
32. Gui,L. and Homer,H. (2012) Spindle assembly checkpoint signalling is uncoupled from chromosomal position in mouse oocytes. *Development*, **139**, 1941–1946.
33. Percival,S.M. and Parant,J.M. (2016) Observing mitotic division and dynamics in a live zebrafish embryo. *J. Vis. Exp.*, **113**, e54218.
34. Tachibana-Konwalski,K., Godwin,J., Borsos,M., Rattani,A., Adams,D.J. and Nasmyth,K. (2013) Spindle assembly checkpoint of oocytes depends on a kinetochore structure determined by cohesin in meiosis I. *Curr. Biol.*, **23**, 2534–2539.